

Influence of offset on osseointegration in cementless total hip arthroplasty: A finite element study

Journal Article**Author(s):**

Meisterhans, Michel; Dimitriou, Dimitris; Fasser, Marie-Rosa; Hoch, Armando; Jud, Lukas; Zingg, Patrick O.

Publication date:

2024-07

Permanent link:

<https://doi.org/10.3929/ethz-b-000662348>

Rights / license:

[Creative Commons Attribution 4.0 International](#)

Originally published in:

Journal of Orthopaedic Research 42(7), <https://doi.org/10.1002/jor.25808>

RESEARCH ARTICLE

Influence of offset on osseointegration in cementless total hip arthroplasty: A finite element study

Michel Meisterhans¹  | Dimitris Dimitriou¹  | Marie-Rosa Fasser^{2,3} |
Armando Hoch¹  | Lukas Jud¹  | Patrick O. Zingg¹

¹Department of Orthopedics, Balgrist University Hospital, University of Zurich, Zurich, Switzerland

²Institute of Biomechanics, Balgrist Campus, ETH Zurich, Zurich, Switzerland

³Spine Biomechanics, Department of Orthopedic Surgery, Balgrist University Hospital, University of Zurich, Zurich, Switzerland

Correspondence

Michel Meisterhans, Department of Orthopaedics, Balgrist University Hospital, Forchstrasse 340, 8008 Zurich, Switzerland.
Email: michel.meisterhans@balgrist.ch

Abstract

Early aseptic loosening is caused by deficient osteointegration of the femoral stem due to increased micromotions and represents a common mode of failure in uncemented total hip arthroplasty (THA). This study hypothesized that a higher femoral offset, a smaller stem size and obesity increase femoral micromotion, potentially resulting in early aseptic loosening. A finite element analysis was conducted based on computed tomography segmented model of four patients who received a THA with a triple-tapered straight stem (Size 1, 3, 6). The influence of femoral stem offset (short neck, standard, lateral), head length (S to XXL), femoral anteversion and obesity during daily activities of fast walking and stair climbing was analyzed. The micromotions for the femoral stem zones were compared to a threshold representing a value above which only partial osseointegration is expected. The minimum femoral offset configuration compared to the maximum offset configuration (short neck stem, S head vs. lateral stem, XXL head) leads to a relative mean micromotion increase of 24% for the upper stem zone. Increasing the body weight (body mass index 30–35 kg/m²) increases the micromotion by 20% for all stem zones. The obese population recorded threshold-exceeding micromotions for stem sizes 1 and 3 for all offset configurations during stair climbing. Higher femoral offset, a smaller stem size, and higher loading due to obesity lead to an increase in micromotion between the prosthesis and proximal femur and represent a risk configuration for impaired osseointegration of a triple-tapered straight stem, especially when these three factors are present simultaneously.

KEYWORDS

cementless total hip arthroplasty, finite element analysis, micromotions, offset, osseointegration

This is an open access article under the terms of the [Creative Commons Attribution](https://creativecommons.org/licenses/by/4.0/) License, which permits use, distribution and reproduction in any medium, provided the original work is properly cited.

© 2024 The Authors. *Journal of Orthopaedic Research*® published by Wiley Periodicals LLC on behalf of Orthopaedic Research Society.

1 | INTRODUCTION

Femoral failures account for more than one-third of all early revisions in primary total hip arthroplasty (THA), with femoral-sided aseptic loosening representing the third most common mode of failure after instability and infection.¹ Whereas in long-term polyethylene wear is mainly held responsible for osteolysis with secondary loosening, early aseptic loosening is caused by deficient osseointegration on the femoral stem.¹⁻³

The stability, or the lack of it, is commonly measured as the amount of micromotion at the interface between the bone and the stem under physiological load.⁴ Large interfacial micromotions reduce the chance of osseointegration, and cause the formation of a fibrous tissue layer at the bone-implant interface,⁵ which may eventually lead to early loosening and failure of the arthroplasty.

The threshold of micromotion, above which a fibrous tissue layer forms, remains unclear. However, a systematic review⁶ showed that interfacial micromotion above 30 µm results in partial ingrowth,^{5,7,8} whereas micromotion exceeding 50–150 µm completely inhibits bone ingrowth.^{5,6,9}

Demographic risk factors such as high body mass index (BMI)¹⁰ and young age¹¹ have been described as risk factors of early aseptic loosening due to higher load on the THA. An association between aseptic loosening and lateralized stem-design has been described by Cantin et al.¹² and partially confirmed by Courtin et al.¹³ reporting symptomatic radiological abnormalities for young patients (<70 years) and small lateralized stems sizes. However, the understanding of why these clinical observations lead to potential early aseptic loosening remains unclear.

This study analyzed the influence of stem osseointegration in cementless THA with a finite element method analyzing the femoral micromotion in different implant combinations for different load conditions. We hypothesized that (1) a higher femoral offset, (2) a smaller stem size, (3) obesity, and (4) higher anteversion of the stem increase femoral micromotion, potentially resulting in early aseptic loosening.

2 | METHODS

2.1 | Study population

Four patients were selected from a different THA study cohort, fulfilling the following criteria: (1) standard straight, rectangular, triple

tapered cementless stem with 80 µm hydroxyapatite (HA) coating (Quadra H, Medacta International SA); (2) preoperative planning with a canal filling, press-fitted femoral stem¹⁴ (stem and head size) was achieved intraoperatively and the postoperative stem alignment did not differ from the planning; (3) symptom-free and radiologically unremarkable at clinical follow-up 5 years postoperatively; (4) a computed tomography (CT) scan was available. The selected study population is shown in Table 1.

2.2 | Model setup

Based on the available CT, image segmentation was performed as described in previous publications^{15,16} using Materialise Mimics (Version 24.0, Materialise NV, Leuven, Belgium). To reduce metallic artifacts in the implant bone interface the cortical bone structure of the proximal femur and the femoral stem were segmented individually (Figure 1A,C). A Matlab toolbox¹⁷ based on the rigid iterative closest point algorithm^{18,19} was used to perform a three-dimensional (3D) registration of the segmented femoral stem and replace it with the corresponding 3D model provided by its manufacturer Medacta (Medacta International SA) to obtain a smooth model surface for an improved mesh quality (Figure 1C). The 3D models of the femoral stem and the cortical shell were imported into Spaceclaim (2020.R2; Spaceclaim Corporation), where a Boolean subtraction was performed between cortical shell and stem to create a cancellous bone volume (Figure 1B). The proximal femur was resected at a length of 180 mm to reduce the required computing power (Figure 1A,D).

2.3 | Simulated factors of interest

To investigate the influence of femoral offset in cementless THA on micromotions, the implanted femoral stem was altered based on the configurations in Tables 1 and 2. Femoral offset was defined as horizontal stem offset plus horizontal head offset and increases with increasing stem size and head length (Tables 2 and 3). To simplify the calculations, the initially planned prosthesis size was left in place and the force vector at the prosthesis taper was shifted accordingly to Table 3 to test different stem and head length configurations (Figure 2B). For each patient the planned,

TABLE 1 Study population overview.

Patient (ID)	Age (years)	Sex (M, F)	Weight (kg)	Height (cm)	BMI (kg/m ²)	Side	Femoral component	Femoral anteversion (°)	Bone-stem contact area (mm ²)
1	80	M	85	175	27.8	Right	Quadra H 6 LAT, L	14	6813
2	64	M	90	173	30.1	Right	Quadra H 3 STD, L	8	5941
3	57	F	73	160	28.5	Right	Quadra H 1 SN STD, M	22	4777
4	42	F	92	170	31.8	Right	Quadra H 3 LAT, M	20	5749

Note: Femoral anteversion was measured according to Stem et al.⁴⁶ Bone-stem contact area in mm² was measured in the developed model.

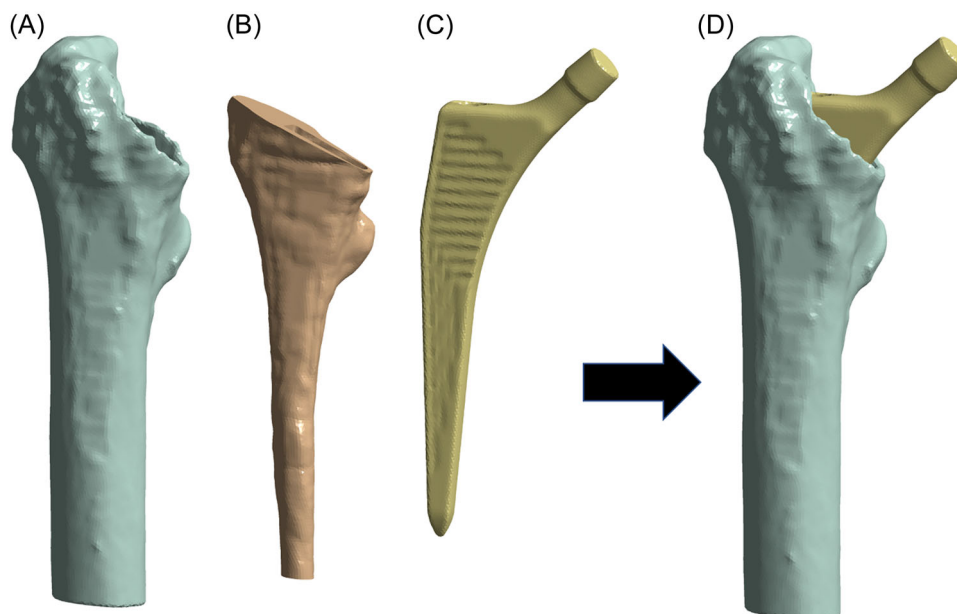


FIGURE 1 Model setup (D) showing cortical shell (A) retrieved by CT-segmentation, followed by cancellous volume (B) created by Boolean subtraction between segmented prosthesis stem and cortical shell. To improve meshing quality the segmented stem was replaced with the original three-dimensional model of the stem (C) provided by the manufacturer.

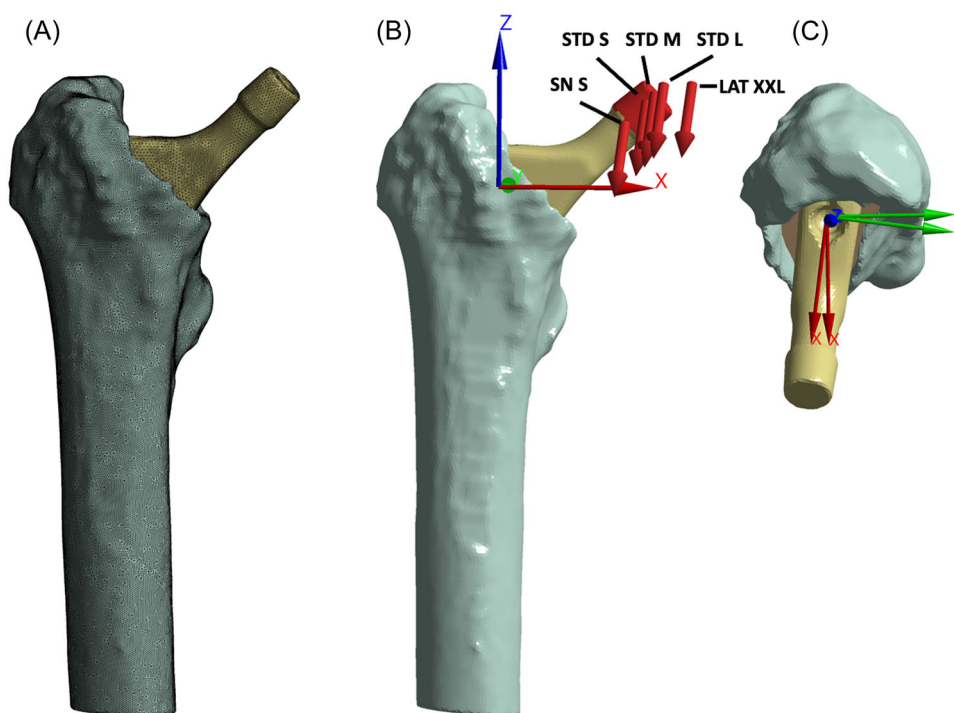


FIGURE 2 (A) Meshed test configuration with resected distal femur based on CT segmentation and implanted femoral stem. (B) Centered the setup with different force vector applications is shown simulating different stem and head configurations for patient no. 2 with planned femoral stem size 3 STD with head length M. (C) The original coordinate system and the stem fixed coordinate system is visible in the axial view.

respectively implanted stem and head configuration was tested as default. One head length smaller and one bigger was tested followed by the minimum femoral offset configuration with a short neck (SN) standard (STD) Quadra H stem with a neck shaft angle

(NSA) of 135° and S head length and the maximum femoral offset configuration with a lateral (LAT) Quadra H stem (NSA of 127°) with XXL head length leading to a horizontal femoral offset difference of 19 mm (Table 3).²⁰

TABLE 2 Stem offset for different stem sizes and types.

	Stem type	Stem size				
		Size 0	Size 1	Size 3	Size 6	Size 10
Stem offset (mm)	STD	40	41	42	44	49
	STD SN	36	37	38	40	45
	LAT	-	45	46	48	-

Note: STD, NSA 135°; STD SN, NSA 135°; LAT, NSA 127°; stem configuration with head length S.

TABLE 3 Femoral offset based on different stem types (stem offset) and head length (head offset) configurations.

	Stem type						
	SN	STD	STD	LAT			
Head length	S	M	M	M	L	XL	XXL
Femoral offset (mm)	0	+3	+6	+11	+13	+16	+19

Note: For Medacta Quadra H stems.³⁰ The short neck standard (SN STD) and standard (STD) stem offer an NSA of 135°, whereas the lateral (LAT) stem has an NSA of 127°.

2.4 | Individual population

Four patients with individual configurations regarding stem size, head length, BMI and stem anteversion (according to Table 1) were tested.

2.5 | Normed population

To reduce the variability of the study population, a normalized population was additionally simulated with a fixed BMI of 30 kg/m² to account for the increasing prevalence of overweight in arthroplasty patients²¹ and anteversion of 12° for all four patient configurations, which will be referenced as “normed” from then on.

2.6 | Obese population

To investigate the influence of obesity, the normed population was additionally tested with a BMI of 35 kg/m².

2.7 | Anteversion

To investigate the influence of stem anteversion on micromotion, Patient 4 was also simulated with 2°, 12°, and 22° anteversion.

2.8 | Finite element analysis and material properties

For the finite element analysis (FEA), Ansys Workbench (Version R1, Ansys Inc.) was used to create a mesh using tetragonal elements with

an approximate element size of 1 and 0.5 mm in the bone-to-implant interface area. An aspect ratio of <4 was recorded for 95% of its elements (Figure 2A). Cortical bone was considered transversely isotropic ($E_x = E_y = 11.5$ GPa, $E_z = 17$ GPa; $\nu_{xy} = 0.51$, $\nu_{xz} = \nu_{yz} = 0.31$ GPa), whereas cancellous bone was modeled as a linear isotropic material property ($E = 2.13$ GPa and $\nu = 0.3$).²² The stem was made of titanium with a modulus of elasticity of 110 GPa and a Poisson ratio of 0.3.²³ In this study, contact between the bone and prosthesis was assumed along the HA coating surfaces of the stem.²³ The used Medacta Quadra H stem has an 80 µm thick HA coating on the whole shaft.²⁰ The stem-bone contact interface was modeled using the augmented Lagrange algorithm with face-to-face contact elements,²⁴ with the prosthesis as the contact body and the cancellous and cortical bone in the femoral cavity as the target body. A frictional contact with press-fit was used to account for the cortical and condensed thin cancellous bone layer in contact with the stem.^{4,25} The press-fit was simulated with an interference of 0.05 mm^{4,25} and the frictional contact with a coefficient set to 0.63.^{23,26} The convergence was checked for micromotion and equivalent stress with a tolerance of 1%.

2.9 | Loading and boundary conditions

FEA was carried out for the static loading conditions defined by Bergmann et al.²⁷ simulating fast walking, the most common physiological activity,²⁸ and stair climbing, which induced high torsional load. The femoral condyles respectively the resected distal femur was assumed to be rigidly constrained in all directions.²³ For fast walking, the applied resultant hip joint contact force was 2.5 × body weight (BW) with a vector direction of 12° in XZ plane and 30° in XY plane.²⁷ For stair climbing, the applied resultant hip joint contact forces were 2.51 × BW with a vector direction of 14° in XZ plane and 46° in XY plane.²⁷ The resultant forces were oriented in a coordinate system defined by Bergmann et al.²⁷ where the z-axis was parallel to the idealized midline of the femur and the x-axis was parallel to the dorsal contour of the femoral condyles in the transverse plane. To simplify force applications for different stem and head configurations the hip joint contact forces were translated in a coordinate system fixed to the stem based on the original coordinate system by rotation around the z-axis depending on the measured stem anteversion of the study subject (Table 2; Figure 2C).

2.10 | Outcome measures

The femoral stem was divided into three zones (upper, middle, and lower) by combining Zone 1, 7, 8 and 14 according to Gruen²⁹ for the upper zone, 2, 6, 9 and 13 for the middle zone and 3, 5, 10 and 12 for the lower zone (Figure 3). For each of these zones, the maximal and mean micromotion (µm) was calculated.³⁰ The calculated micromotion values were compared to a threshold of 30 µm, respectively, 150 µm representing a value above which only partial bony integration, respectively, no bony integration are expected.^{5–8}

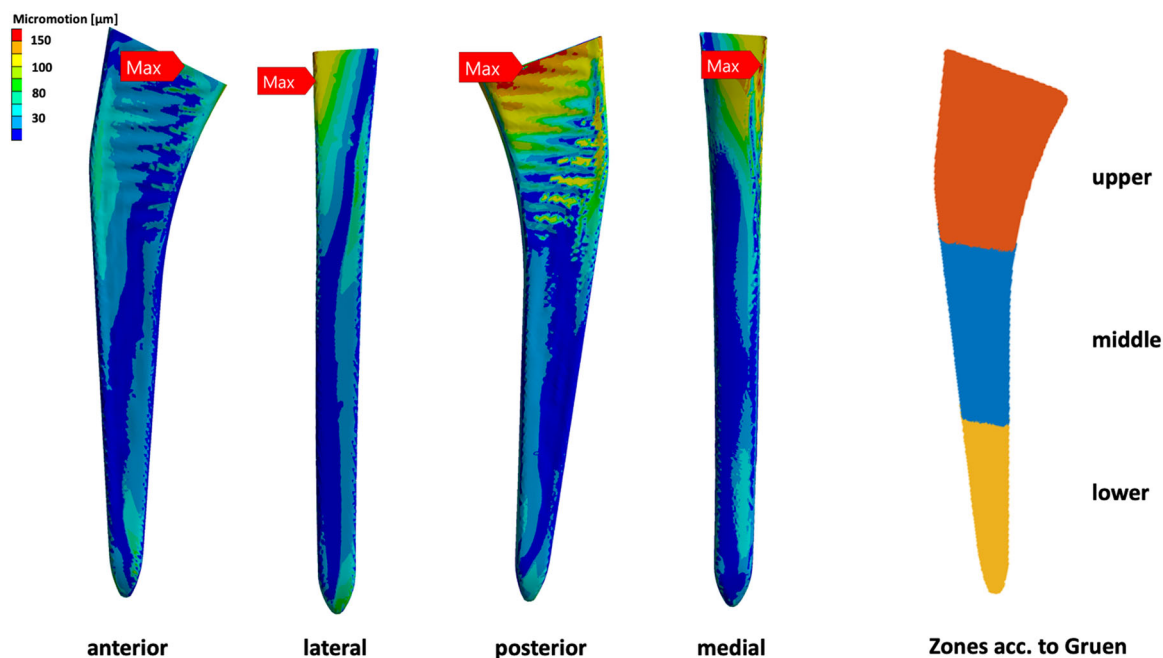


FIGURE 3 Typical micromotion distribution for the contact area of the stem in different views. To the right the division of the three different zones according to Gruen.²⁹

3 | RESULTS

For all tested configurations the maximum micromotion was recorded in the posteromedial area of the upper stem zone during stair climbing as well as fast walking as representatively shown in Figure 3. For the middle and lower stem zones, the influence of offset on relative micromotion decreases slightly. A decrease in the femoral offset of one head length leads to 5% of mean micromotion reduction for LAT stems (4% for STD stems) in the upper stem zone, an increase of offset by one head length leads to 4% of mean micromotion increase for the upper stem zone for LAT stems (3% for STD stems). The minimum femoral offset configuration compared to the maximum offset configuration (SN stem with S head to LAT stem with XXL head) leads to a relative mean micromotion increase of 24% for the upper stem zone (Table 4). Increasing the BW (BMI 30–35 kg/m²) increases the micromotion by 20% for all stem zones (Table 4), corresponding to an approximative linear correlation if the two patients from the individual population with a BMI <30 kg/m² are considered. When comparing the micromotions of patients with stem size 3 to patients with stem size 1, an increase of 12% in the upper stem area is recorded. When comparing patients with stem size 6 to size 3, an increase of 19% in the upper stem area is recorded (Table 4). The femoral stem-to-bone contact area for the different configurations is presented in Table 1.

3.1 | Individual population

For the individual configurations (Figure 4) only Patient 4 in the maximum offset configuration (Quadra H size 3, LATERAL, XXL head)

and planned + 1 configuration (Quadra H size 3, LATERAL, XL head) recorded a maximum (168 µm, respectively, 156 µm) and mean (33 ± 22 µm, respectively, 30 ± 19 µm) micromotion of the upper stem area exceeding the threshold of osteointegration for stair climbing. All other configurations recorded mean micromotion values below the thresholds.

3.2 | Normed population

To allow for a more parametric comparison, the BW and the anteversion of the stem were standardized for all four patients (BMI 30 kg/m², 12° anteversion). Patients 3 and 4 recorded a maximum (158 µm, respectively, 159 µm) and mean (33 ± 19 µm, respectively, 31 ± 21 µm) micromotion for the maximum offset configuration (LATERAL stem size 1, respectively, 3, XXL head) exceeding the threshold for osteointegration for the upper stem zone during stair climbing (Figure 5).

3.3 | Obese population

An increase in BW to a BMI of 35 kg/m² leads to an exceed in maximum and mean micromotion thresholds for Patients 3 and 4 for all offset configurations during stair climbing (Figure 6). Patient 3 in maximum offset configuration (Quadra H size 1, LATERAL, XXL head) exceeded the maximum threshold for osteointegration even during fast walking with a micromotion maximum of 159 µm and mean of 30 ± 17 µm.

TABLE 4 Relative mean micromotion in % for normed configurations.

	Relative micromotion in %		Max offset	BMI (kg/m ²)	Stem size	Anteversion	
	- Head size STD (LAT)	+ Head size STD (LAT)					
Stem area	planned → planned - 1	planned → planned + 1	SN S → LAT XXL	30 → 35	3 → 1	6 → 3	2° → 22°
Upper zone	-4% (-5%)	+3% (+4%)	+24%	+20%	+12%	+19%	+3%
Middle zone	-3% (-4%)	+3% (+4%)	+21%	+20%	+23%	+18%	+6%
Lower zone	-2% (-3%)	+2% (+3%)	+16%	+20%	+21%	+21%	-5%

Note: Showing the influence of head length increase/decrease, difference between maximum and minimum offset configuration (SN stem with S head to LAT stem with XXL head), influence of body weight increase (BMI 30/35), influence of different stem sizes (comparing different normed patients with different stem sizes) and influence of stem anteversion for upper, middle, and lower stem zones.

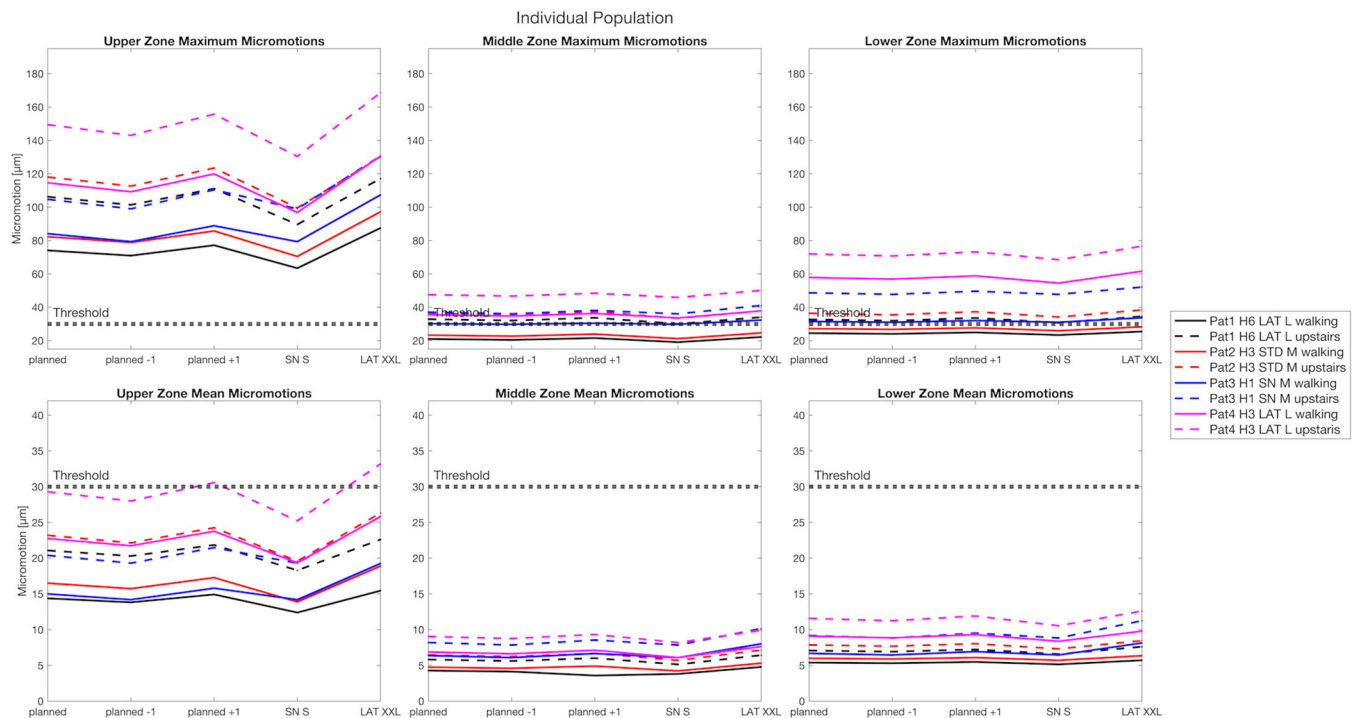


FIGURE 4 Micromotion for the different stem zones plotted for the individual population according to Table 1 during fast walking (solid lines) and stair climbing (dashed lines). Upper row: maximum recorded micromotion. Lower row: Mean micromotion.

3.4 | Anteversion

When analyzing the different stem anteversions (2°, 12°, and 22°), a trend for a slight increase in micromotion with increased femoral anteversion is identified. An increase of mean micromotions for the upper stem area of 3% for 22° compared to 2° of anteversion (6% for middle and -5% for lower stem area) was recorded (Table 4; Figure 7).

4 | DISCUSSION

The main findings of this study are that a high femoral offset, a smaller stem size, and higher loading due to obesity (BMI 35 kg/m²) lead to an increase in micromotion between the standard straight

stem and proximal femur and might be associated with an osseointegration failure. Stair climbing leads to a significantly higher micromotion than walking due to the higher lever arms. The anteversion of the stem, on the other hand, has no conclusive influence on micromotion.

Recent evidence supports that lateralized femoral stems might be associated with increased aseptic loosening. Courtin et al.¹³ showed in a retrospective study with 172 THA that young patients with a small lateralized stem have a hazard ratio of 12.5 for integration abnormalities on postoperative x-rays. Lateralized stems had a 4% rate of revision for aseptic loosening. However, in their study, the influence of different head lengths was not respected. In an analysis of midterm results, Cantin et al.¹² partially confirmed the results in a retrospective cohort study showing a higher risk for aseptic loosening with lateralized stems compared to standard stems.

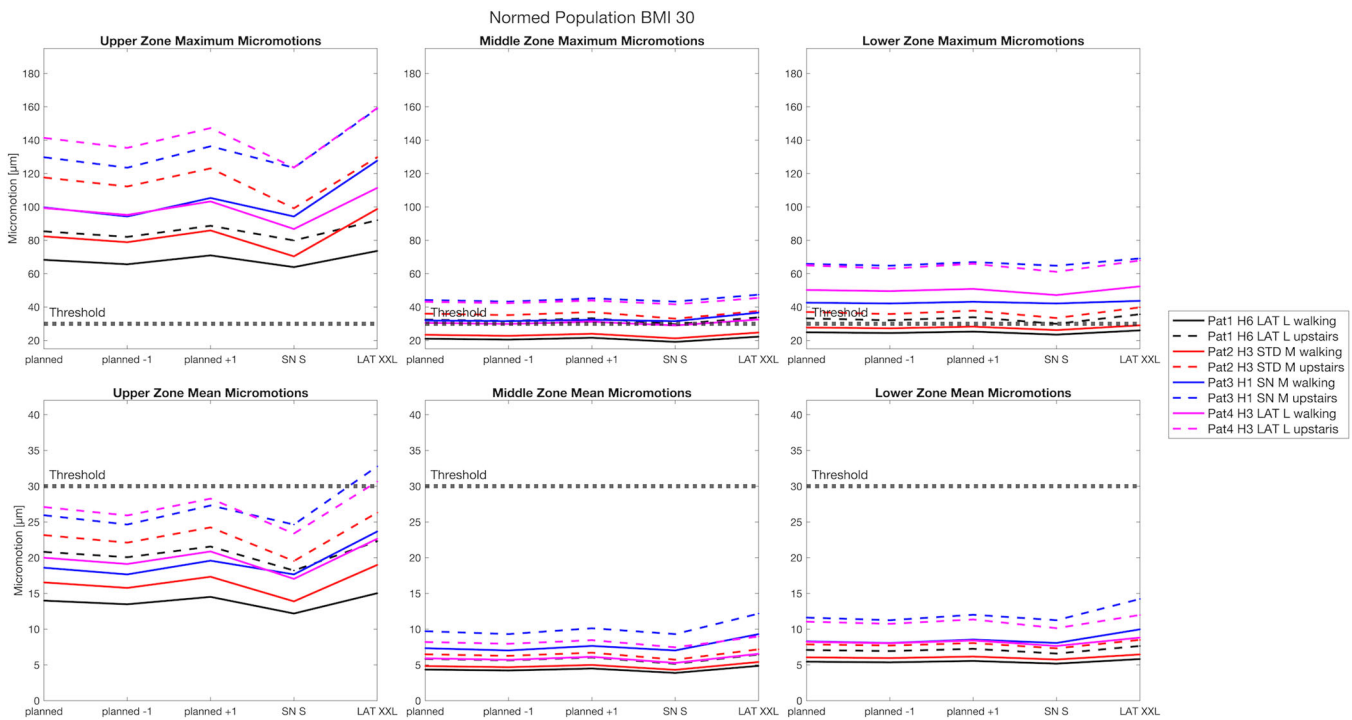


FIGURE 5 Micromotion for normed population (BMI 30 kg/m², anteversion 12°) during fast walking (solid lines) and stair climbing (dashed lines). Upper row: maximum recorded micromotion. Lower row: mean micromotion.

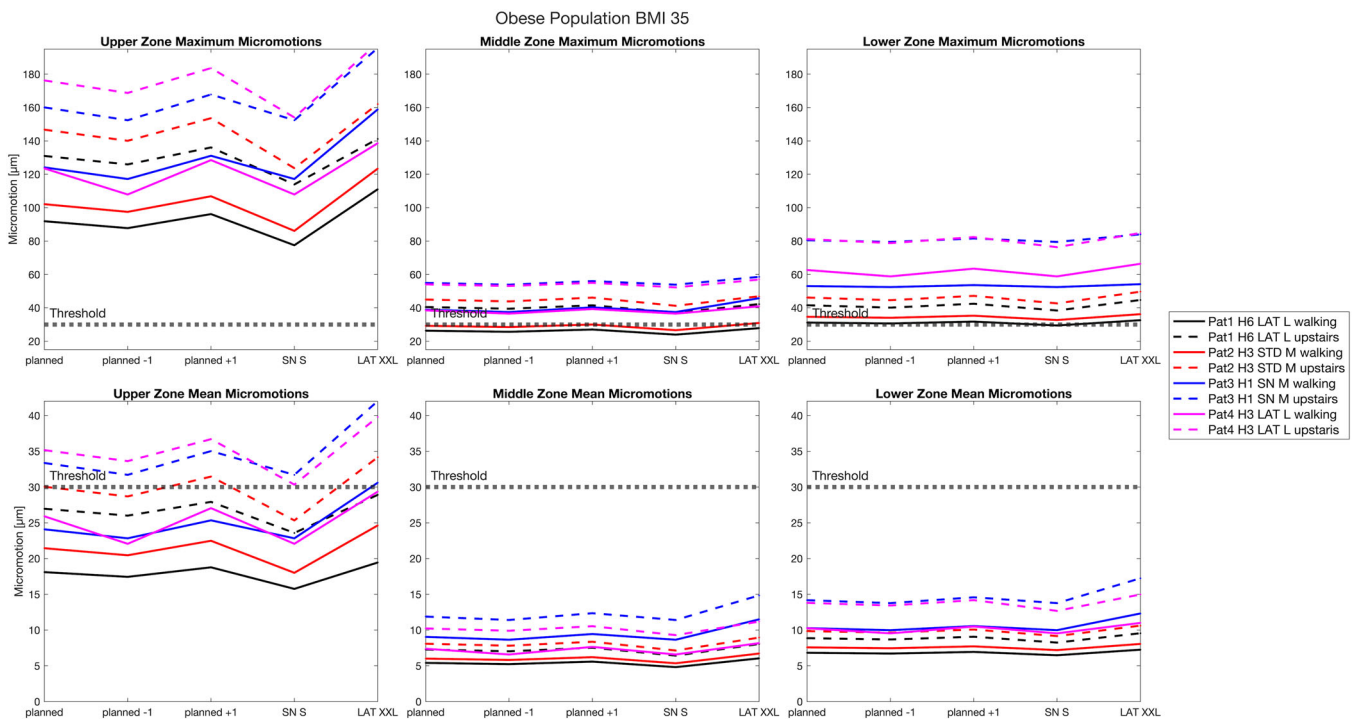


FIGURE 6 Micromotion for obese population (BMI 35 kg/m², anteversion 12°) during fast walking (solid lines) and stair climbing (dashed lines). Upper row: maximum recorded micromotion. Lower row: Average micromotion.

This study showed that after restoring the anatomical offset in THA according to preoperative planning, 5% of micromotion reduction is achieved by choosing one head length smaller as planned (for LAT stem, 4% for STD stem), whereas 4% micromotion increase is created

by choosing one head length bigger as planned (for LAT stem, 3% for STD stem). If the anatomical offset is disregarded, a micromotion reduction of up to 24% can be achieved with a minimal prosthetic offset configuration (SN stem, S head vs. LAT stem, XXL head).

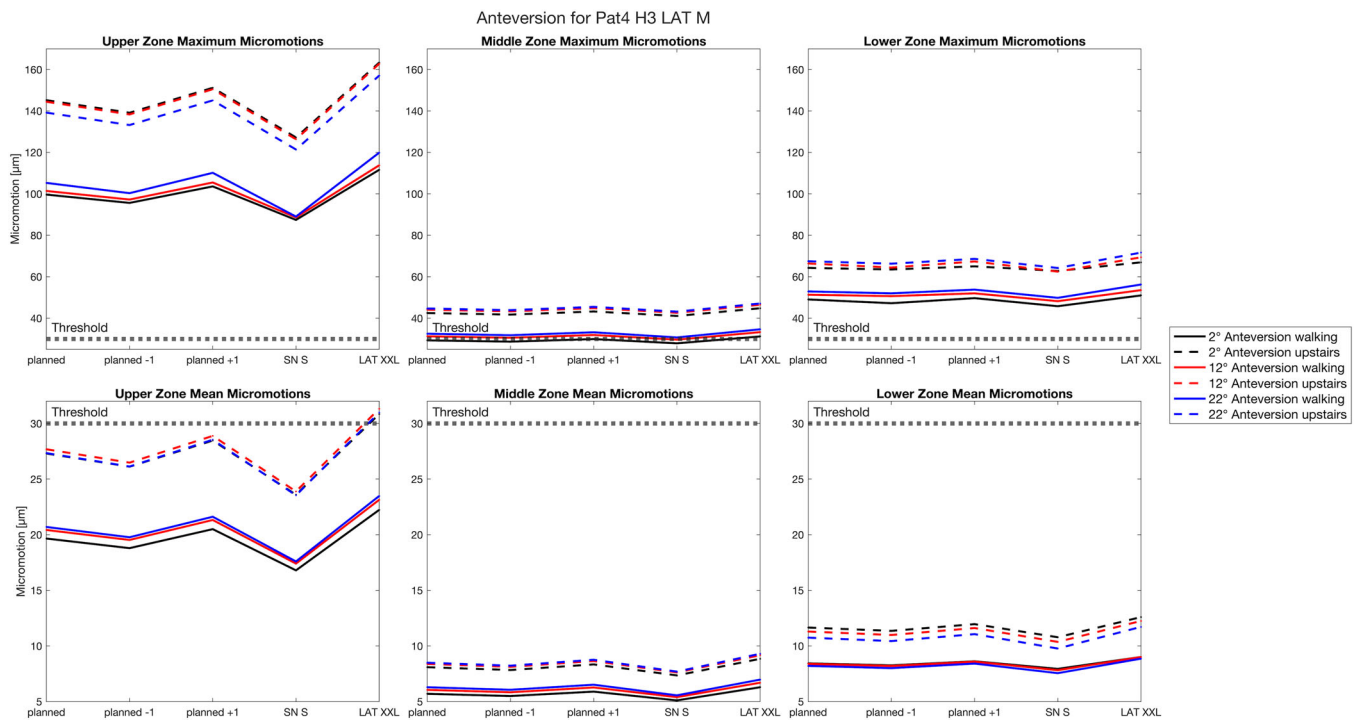


FIGURE 7 Micromotion for different anteversions (2° , 12° , and 22°) for Patient 4 with Quadra H size 3 for different offset configurations during fast walking (solid lines) and stair climbing (dashed lines) is shown. Upper row: maximum recorded micromotion. Lower row: Mean micromotion.

However, the quality of offset reconstruction is known to be crucial to achieve a desirable abductor function.³¹ Medialisation of the center of rotation in favor of a greater femoral offset has been shown to correlate with an increased range of abduction and greater abductor strength and reduced joint reaction forces.³² On the other hand, high femoral offset may lead to stress on prosthetic components as well as their fixation.³³ The results of the study do not aim to guide surgeons to choose implants with a small offset, but rather to restore the anatomical offset in THA and to be aware of the influence on micromotion and possibly increased risk of aseptic loosening in case of high offset configurations or overcorrections.

Peak micromotions in the femoral stem/bone interface typically occur in the posteromedial region during activities of daily living. Al-Dirini et al.³⁴ conducted a FEA on a cohort of 31 femora to investigate the femoral micromotions for standard, lateral and coxa vara stem configurations for walking and stair climbing, recording the highest peak and median micromotions during both activities for the lateral stem configuration. Abdul Kadir et al.⁴ showed with a FEA model correlated to an in vitro micromotion experiment on four cadavers that an interference fit around $50\ \mu\text{m}$ in the FEA model corresponds most closely to the situation of a press-fit of an uncemented stem and reported micromotions in the upper stem zone of $50\text{--}150\ \mu\text{m}$. The range of micromotions predicted in this study using a validated interference fit of $50\ \mu\text{m}$ is comparable to those found in the reported FEA studies locating the peak micromotion in the posterior medial area of the stem. As expected, stair climbing

produces more motion at the bone-implant interface than fast walking due to higher lever arms on the proximal femur.³⁵

Reimeringer et al.²³ showed in a FEA study an increase in micromotion for shorter straight stems as well as for shorter curved stems without altering the femoral offset of the stems due to reduced interface contact area. Although the horizontal femoral offset increases with prosthesis size (2 mm from size 1 to size 3), this study demonstrated that the influence of the interface contact area on micromotions is more relevant. Thus, patient 3 (stem size 1) shows higher average micromotions in all 3 femoral zones for the normalized test configurations for the minimum and maximum offset configurations (SN S and LAT XXL) compared to patients 2 and 4 (stem size 3; Figure 5). Therefore, the anatomical offset should be restored by selecting the largest possible stem to provide a canal filling press-fit and increase implant-to-bone contact taking into account the anatomical conditions and risk of intraoperative periprosthetic fracture.

The results of this study pertain to uncemented triple-tapered straight stems type B2 according to Radaelli et al.³⁶ This straight stem category includes not only the Medacta Quadra shaft used in this study but also commonly used shafts such as the Corail from J&J DePuy Synthes, Avenir from Zimmer Biomet, or Polarstem from Smith & Nephew. Reimeringer et al.²³ illustrated through FEA that, for short curved stems (B3 according to Radaelli et al.³⁶), there was an increase in micromotions as shaft lengths decreased suggesting that the findings of this study might also be applicable to shaft designs deviating from triple-tapered straight stems.

Obesity is independently associated with early primary THA failure for aseptic loosening.¹⁰ In 2011, 35% of US adults were classified as obese (BMI > 30 kg/m²) and this prevalence continues to increase.³⁷ Goodnough et al.¹⁰ reported an odds ratio of 2.31 for THA failure for aseptic loosening before 5 years for obese patients compared to the nonobese control group. Our results might explain these findings as a 20% micromotion increase is shown for all stem zones due to a BMI increase from 30 to 35 kg/m² showing a linear correlation between micromotions and BMI increase. For the obese testing configurations, two patients recorded micromotions above the osteointegration threshold for all tested offset configurations predicting aseptic loosening (Figure 6).

Biologically, osseointegration starts with woven bone formation, followed by a period of remodeling to lamellar bone in response to mechanical loading, which starts around 6–8 weeks after implantation and can take up to a month to complete.³⁸ The following implant and external factors were associated with higher levels of tolerated micromotions and successful osseointegration: HA coating, infrequent loading and a rest period following initial loading.⁶ Goodman et al. showed that oscillatory motions up to 750 µm once a day would allow successful osseointegration, while the same motions twice a day would not, emphasizing the effect of loading duration.³⁹ Therefore, activities as stair climbing for high-risk configurations (high femoral offset, small stem size, and obesity) could be tolerable if not conducted frequently during early postoperative rehabilitation phase. In a systematic review, a positive correlation between tolerable micromotions to achieve osteointegration and contact-area of bone to implant was shown,⁶ however, it remains unclear how much area of osteointegration on the femoral stem is required to prevent early loosening.

Accordingly, in configurations of high offset, small prosthesis, and obese patients, postoperative partial weight bearing may be considered to prevent early aseptic loosening by reducing the micromotion below the threshold to allow osteointegration.

The direct anterior approach has recently gained popularity owing to smaller stem sizes, modified instruments and its perception as a minimally-invasive procedure and it is the approach of choice at our institution for primary THA. However, some studies report a risk of excessive femoral anteversion compared to a posterior approach.^{40,41} Our study could not show a clear correlation between increased femoral anteversion and micromotion and thus possible early aseptic loosening.

This study presents some limitations. Although the behavior of human bone is anisotropic heterogeneous,⁴² material properties used to characterize the composite bone have been defined as transversely isotropic, with Young's moduli for cortical and cancellous bones extracted from the literature. Baca et al.⁴³ found that the global displacement of the femur was influenced by bone material properties assignment; the use of isotropic homogeneous properties underestimated this displacement. Moreover, in this study, the press-fit contact between the bone and prosthesis was assumed along the entire HA coating of the stem. However, Wu et al.⁴⁴ found that only 60% of the stem–bone interface was really in contact in a cadaveric study, whereas Howard et al.⁴⁵ found using CT measurement that

only 43% of the stem–bone interface was really in contact. Park et al.⁴⁶ underlined that gaps located in the upper zone can have a pronounced effect on the primary stability of a THA stem. This indicates that micromotions found in the present study most probably underestimate the real condition. Furthermore, the anteversion of the stem was not changed by rotation of the stem relative to the femur, but by rotation of the resulting force vector on the prosthetic taper. Like most finite element studies without in vitro correlation, simulated physiological activities are defined as static load cases, whereas in vitro studies can simulate dynamic physiological load cases. The influence of different leg lengths and thus different leverage ratios was not considered in this study, but the influence of body size was indirectly considered by BMI. Nevertheless, this study is valid for comparing the numerical solutions for different offset configurations for triple-tapered straight stems.

5 | CONCLUSION

Higher femoral offset, a smaller stem size, and higher loading due to obesity lead to an increase in micromotion between the prosthesis and proximal femur and represent a risk configuration for impaired osteointegration of a triple-tapered straight stem, especially when these three factors are present simultaneously. An increase in BMI of five points alone leads to a relative increase in micromotion of 20% in all stem zones. In these risk configurations, initial partial weight bearing may be considered to reduce micromotion and allow osseointegration of the implant.

AUTHOR CONTRIBUTIONS

Michel Meisterhans: Conception, writing, revising, creating CAD models, performing FEA, data read-out and interpretation. **Dimitris Dimitriou:** Conception, writing, revising. **Marie-Rosa Fasser:** Creating CAD models, data read-out, revising. **Armando Hoch:** Conception, revising. **Lukas Jud:** Conception, revising. **Patrick O. Zingg:** Conception, writing, revising. All authors approved the final manuscript.

ACKNOWLEDGMENTS

The authors declare that no funds, grants, or other support were received during the preparation of this manuscript. The authors thank Medacta International SA (Castel San Pietro, Switzerland) for the supply of the 3D models for the Quadra H hip stems used in this study. Patrick O. Zingg is a paid consultant for Medacta International SA. The remaining authors declare that they have no known competing financial interests or personal relationships that could appear to have influenced the work reported in this paper. Open access funding provided by Universitat Zurich.

ORCID

Michel Meisterhans  <http://orcid.org/0000-0002-2478-3877>

Dimitris Dimitriou  <http://orcid.org/0000-0002-9558-7080>

Armando Hoch  <http://orcid.org/0000-0002-9600-4190>

Lukas Jud  <http://orcid.org/0000-0001-8128-3927>

REFERENCES

1. Melvin JS, Karthikeyan T, Cope R, Fehring TK. Early failures in total hip arthroplasty—a changing paradigm. *J Arthroplasty*. 2014;29:1285-1288.
2. Apostu D, Lucaciu O, Berce C, Lucaciu D, Cosma D. Current methods of preventing aseptic loosening and improving osseointegration of titanium implants in cementless total hip arthroplasty: a review. *J Int Med Res*. 2018;46:2104-2119.
3. Havelin L, Espehaug B, Vollset S, Engesaeter L. Early aseptic loosening of uncemented femoral components in primary total hip replacement. A review based on the Norwegian Arthroplasty Register. *J Bone Joint Surg Br*. 1995;77:11-17.
4. Abdul-Kadir MR, Hansen U, Klabunde R, Lucas D, Amis A. Finite element modelling of primary hip stem stability: the effect of interference fit. *J Biomech*. 2008;41:587-594.
5. Pilliar R, Lee J, Maniopoulos C. Observations on the effect of movement on bone ingrowth into porous-surfaced implants. *Clin Orthop Relat Res*. 1986;108-113.
6. Kohli N, Stoddart JC, van Arkel RJ. The limit of tolerable micromotion for implant osseointegration: a systematic review. *Sci Rep*. 2021;11:10797.
7. Engh CA, O'Connor D, Jasty M, McGovern TF, Bobyn JD, Harris WH. Quantification of implant micromotion, strain shielding, and bone resorption with porous-coated anatomic medullary locking femoral prostheses. *Clin Orthop Relat Res*. 1992;(285):13-29.
8. Vandamme K, Naert I, Geris L, Sloten JV, Puers R, Duyck J. Histodynamics of bone tissue formation around immediately loaded cylindrical implants in the rabbit. *Clin Oral Implants Res*. 2007;18:471-480.
9. Soballe K, Hansen E, Brockstedt-Rasmussen H, Bunger C. Hydroxyapatite coating converts fibrous tissue to bone around loaded implants. *J Bone Joint Surg Br*. 1993;75:270-278.
10. Goodnough LH, Finlay AK, Huddleston 3rd JI, Goodman SB, Maloney WJ, Amanatullah DF. Obesity is independently associated with early aseptic loosening in primary total hip arthroplasty. *J Arthroplasty*. 2018;33:882-886.
11. Münger P, Röder C, Ackermann-Liebrich U, Busato A. Patient-related risk factors leading to aseptic stem loosening in total hip arthroplasty: a case-control study of 5,035 patients. *Acta Orthop*. 2006;77:567-574.
12. Cantin O, Viste A, Desmarchelier R, Besse JL, Fessy MH. Compared fixation and survival of 280 lateralised vs 527 standard cementless stems after two years (1-7). *Orthop Traumatol Surg Res*. 2015;101:775-780.
13. Courtin C, Viste A, Subtil F, Cantin O, Desmarchelier R, Fessy MH. Cementless lateralized stems in primary THA: mid-term survival and risk factors for failure in 172 stems. *Orthop Traumatol Surg Res*. 2017;103:15-19.
14. Colombi A, Schena D, Castelli CC. Total hip arthroplasty planning. *EFORT Open Rev*. 2019;4:626-632.
15. Fucntese SF, Meier P, Jud L, et al. Accuracy of 3D-planned patient specific instrumentation in high tibial open wedge valgisation osteotomy. *J Exp Orthop*. 2020;7:7.
16. Lorensen WE, Cline HE. Marching cubes: a high resolution 3D surface construction algorithm. *ACM SIGGRAPH Comput Graph*. 1987;21:163-169.
17. Mathworks Inc. Rigid ICP registration. MATLAB Central File Exchange. Mathworks Inc. 2022.
18. Gruen A, Akca D. Least squares 3D surface and curve matching. *ISPRS J Photogramm Remote Sens*. 2005;59:151-174.
19. Besl PJ, McKay ND. Method for registration of 3-D shapes. *IEEE Trans Pattern Anal Mach Intell*. 1992;14(2):239-256.
20. Medacta International SA. Quadra System, Technical Data. Medacta International SA.
21. Fehring TK, Odum SM, Griffin WL, Mason JB, McCoy TH. The obesity epidemic. *J Arthroplasty*. 2007;22:71-76.
22. Kayabasi O, Ekici B. The effects of static, dynamic and fatigue behavior on three-dimensional shape optimization of hip prosthesis by finite element method. *Mater Des*. 2007;28:2269-2277.
23. Reimeringer M, Nuño N, Desmarais-Trépanier C, Lavigne M, Vendittoli PA. The influence of uncemented femoral stem length and design on its primary stability: a finite element analysis. *Comput Methods Biomech Biomed Eng*. 2013;16:1221-1231.
24. Viceconti M, Muccini R, Bernakiewicz M, Baleani M, Cristofolini L. Large-sliding contact elements accurately predict levels of bone-implant micromotion relevant to osseointegration. *J Biomech*. 2000;33:1611-1618.
25. Bah MT, Shi J, Heller MO, et al. Inter-subject variability effects on the primary stability of a short cementless femoral stem. *J Biomech*. 2015;48:1032-1042.
26. Grant JA, Bishop NE, Götzén N, Sprecher C, Honl M, Morlock MM. Artificial composite bone as a model of human trabecular bone: the implant-bone interface. *J Biomech*. 2007;40:1158-1164.
27. Bergmann G, Deuretzbacher G, Heller M, et al. Hip contact forces and gait patterns from routine activities. *J Biomech*. 2001;34:859-871.
28. Morlock M, Schneider E, Bluhm A, et al. Duration and frequency of every day activities in total hip patients. *J Biomech*. 2001;34:873-881.
29. Gruen TA, McNeice GM, Amstutz HC. "Modes of failure" of cemented stem-type femoral components: a radiographic analysis of loosening. *Clin Orthop Relat Res*. 1979;141:17-27.
30. Ostbyhaug PO, Klaksvik J, Romundstad P, et al. Primary stability of custom and anatomical uncemented femoral stems: a method for three-dimensional in vitro measurement of implant stability. *Clin Biomech*. 2010;25:318-324.
31. Asayama I, Naito M, Fujisawa M, Kambe T. Relationship between radiographic measurements of reconstructed hip joint position and the Trendelenburg sign. *J Arthroplasty*. 2002;17:747-751.
32. McGrory B, Morrey B, Cahalan T, An K, Cabanela M. Effect of femoral offset on range of motion and abductor muscle strength after total hip arthroplasty. *J Bone Joint Surg Br*. 1995;77:865-869.
33. Sakalkale DP, Sharkey PF, Eng K, Hozack WJ, Rothman RH. Effect of femoral component offset on polyethylene wear in total hip arthroplasty. *Clin Orthop Relat Res*. 2001;388:125-134.
34. Al-Dirini RMA, Martelli S, Huff D, et al. Evaluating the primary stability of standard vs lateralised cementless femoral stems—a finite element study using a diverse patient cohort. *Clin Biomech*. 2018;59:101-109.
35. Heller MO, Bergmann G, Kassi JP, Claes L, Haas NP, Duda GN. Determination of muscle loading at the hip joint for use in pre-clinical testing. *J Biomech*. 2005;38:1155-1163.
36. Radaelli M, Buchalter DB, Mont MA, Schwarzkopf R, Hepinstall MS. A new classification system for cementless femoral stems in total hip arthroplasty. *J Arthroplasty*. 2023;38:502-510.
37. Ogden CL, Carroll MD, Kit BK, Flegal KM. Prevalence of childhood and adult obesity in the United States, 2011-2012. *JAMA*. 2014;311:806-814.
38. Kohli N, Ho S, Brown SJ, et al. Bone remodeling in vitro: where are we headed? *Bone*. 2018;110:38-46.
39. Goodman S, Wang JS, Doshi A, Aspenberg P. Difference in bone ingrowth after one versus two daily episodes of micromotion: experiments with titanium chambers in rabbits. *J Biomed Mater Res*. 1993;27:1419-1424.
40. Watanabe K, Mitsui K, Usuda Y, Nemoto K. An increase in the risk of excessive femoral anteversion for relatively younger age and types of femoral morphology in total hip arthroplasty with direct anterior approach. *J Orthop Surg*. 2019;27:230949901983681.
41. Kobayashi H, Homma Y, Baba T, et al. Surgeons changing the approach for total hip arthroplasty from posterior to direct anterior

- with fluoroscopy should consider potential excessive cup anteversion and flexion implantation of the stem in their early experience. *Int Orthop*. 2016;40:1813-1819.
42. Wirtz DC, Schiffers N, Pandorf T, Radermacher K, Weichert D, Forst R. Critical evaluation of known bone material properties to realize anisotropic FE-simulation of the proximal femur. *J Biomech*. 2000;33:1325-1330.
 43. Baca V, Horak Z, Mikulenka P, Dzupa V. Comparison of an inhomogeneous orthotropic and isotropic material models used for FE analyses. *Med Eng Phys*. 2008;30:924-930.
 44. Wu L, Hahne HJ, Hassenpflug J. The dimensional accuracy of preparation of femoral cavity in cementless total hip arthroplasty. *J Zhejiang Univ Sci A*. 2004;5:1270-1278.
 45. Howard JL, Hui AJ, Bourne RB, McCalden RW, MacDonald SJ, Rorabeck CH. A quantitative analysis of bone support comparing cementless tapered and distal fixation total hip replacements. *J Arthroplasty*. 2004;19:266-273.
 46. Park Y, Choi D, Hwang DS, Yoon YS. Statistical analysis of interfacial gap in a cementless stem FE model. *J Biomech Eng*. 2009;131:021016.

How to cite this article: Meisterhans M, Dimitriou D, Fasser M-R, Hoch A, Jud L, Zingg PO. Influence of offset on osseointegration in cementless total hip arthroplasty: a finite element study. *J Orthop Res*. 2024;42:1566-1576. doi:10.1002/jor.25808